NUMERICAL MATHEMATICS: Theory, Methods and Applications
Numer. Math. Theor. Meth. Appl., Vol. **1**, No. 4, pp. 357-382 (2008)

A Second-Order Method for the Electromagnetic Scattering from a Large Cavity

Yingxi Wang, Kui Du and Weiwei Sun*

Department of Mathematics, City University of Hong Kong, Hong Kong.

Received 18 August, 2007; Accepted (in revised version) 25 June, 2008

Abstract. In this paper, we study the electromagnetic scattering from a two dimensional large rectangular open cavity embedded in an infinite ground plane, which is modelled by Helmholtz equations. By introducing nonlocal transparent boundary conditions, the problem in the open cavity is reduced to a bounded domain problem. A hypersingular integral operator and a weakly singular integral operator are involved in the TM and TE cases, respectively. A new second-order Toeplitz type approximation and a second-order finite difference scheme are proposed for approximating the hypersingular integral operator on the aperture and the Helmholtz in the cavity, respectively. The existence and uniqueness of the numerical solution in the TE case are established for arbitrary wavenumbers. A fast algorithm for the second-order approximation is proposed for solving the cavity model with layered media. Numerical results show the second-order accuracy and efficiency of the fast algorithm. More important is that the algorithm is easy to implement as a preconditioner for cavity models with more general media.

AMS subject classifications: 78M20, 65N22, 65N06

Key words: Electromagnetic scattering, Helmholtz equation, fast algorithm, Toeplitz matrix, second-order method.

1. Introduction

Electromagnetic scattering is one of the most competitive areas in both mathematical and engineering communities comprising of wide range of applications, such as radar, remote sensing, geoelectromagnetics, bioeletromagnetics, antennas, wireless communication, optics and high-frequency/high-speed circuits. In this paper, we are mainly concerned with the electromagnetic scattering from a two-dimensional large open cavity embedded in an infinite ground plane. The geometry of the cavity is shown in Fig. 1. We assume that the ground plane and the walls of the open cavity are perfect electric conductors (PEC), and the interior of the open cavity is filled with non-magnetic materials which may be inhomogeneous. The half-space above the ground plane is filled with a homogeneous, linear

*Corresponding author. *Email addresses:* yxwang@math.cityu.edu.hk (Y. Wang), kuidumath@yahoo.com (K. Du), maweiw@math.cityu.edu.hk (W. Sun)

 ©2008 Global-Science Press

and isotropic medium. In this setting, the electromagnetic scattering by the cavity is governed by the Helmholtz equations along with Sommerfeld's radiation conditions imposed at infinity.

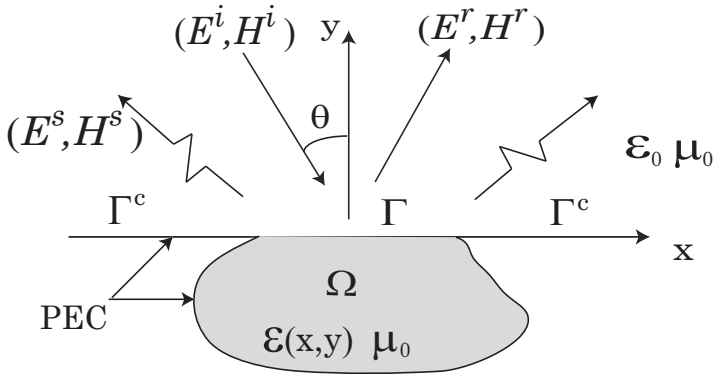

Figure 1: The geometry of the cavity.

Recently, the large cavity problem has attracted much attention because of its significant industrial and military applications. Examples of cavities include jet engine inlet ducts, exhaust nozzles and cavity-backed antennas. The Radar Cross Section (RCS) is an important physical parameter that characterizes scattering by a cavity. Therefore, accurate prediction of the RCS of the cavity is very necessary due to its dominance to the target's overall RCS. However, the accurate computation is especially difficult due to the highly oscillatory nature of the fields when the cavity is large compared to the wavelength of the fields. One often uses finer meshes or higher-order numerical approximations to achieve the better accuracy. In this paper, we intend to develop a second-order method for cavity models and corresponding fast algorithms when the medium inside the rectangular cavity is vertically layered.

In many practical applications, one is interested in the cavity problem with either a large wavenumber k or a large diameter a of the computational domain, which leads to the large "ka" numbers. A straight-forward change of coordinates yields the equivalence of large wavenumbers and large cavity problems. For convenience, without loss of generalities, we focus primarily on large wavenumber problems in our discussion. There are several difficulties for solving the problem with a large wavenumber. One lies in the fact that the solution for a large wavenumber is highly oscillatory. Also, it is well known that error estimates strongly depend upon the wavenumber. Babuska and Sauter [4] showed that for a related model problem, the ratio of the error of the Galerkin solution and the error of the best approximation tends to infinity as the wavenumber increases. Aziz et al. [3] pointed out that the condition "k^2h small" would be required to ensure that the error of the linear FEM solution has the same magnitude as the error of the best approximation, where h is the mesh size. Moreover, approximations of models with large wavenumbers always result in a large, sparse, symmetric, non-Hermitian, indefinite and ill-conditioned discrete system, for which direct methods are extremely expensive and classical iterative algorithms are slowly convergent or even fail to converge.

A variety of numerical methods have been developed to solve the open cavity problems, which include the finite difference method [5,19], the moment method [17,20], the finite element method [8, 12], the boundary element method [7, 24], and hybrid methods [10,13,24]. A detailed discussion and additional references can be found in [2,8]. An important step for solving the open cavity problem is to introduce transparent boundary conditions on the aperture of the cavity. This reduces the infinite domain problems to finite domain problems, which in turn can be solved by classical numerical approximation. More recently, a time-domain finite element method and analysis have been presented in [16]. The time-dependent scattering problem was discretized in time by Newmark's scheme. An important issue in the cavity model is to solve the large scale ill-conditioned system. Liu and Jin [12] proposed a preconditioner based on a physical approximation, which is constructed from the finite element method using an absorbing boundary condition (ABC) on the aperture of the cavity. The system corresponding to the preconditioner is solved either by a direct method or by an iterative method. Bao and Sun [5] explored a fast algorithm of a first-order approximation to the cavity model, where the cavity is a rectangle filled with layered media. In the fast algorithm, the FFT-sine transform in the x-direction and Gaussian elimination along the y-direction are used to reduce the global system to an aperture system that in turn is solved by a preconditioning iterative algorithm. The computational complexity of their algorithm is proportional to the number of unknowns.

Numerical approximations to the cavity model consist of two parts: the approximation to the Helmholtz equation defined in the cavity and the approximation to the nonlocal hypersingular/weakly singular transparent boundary conditions on the aperture. The structure of the discrete nonlocal boundary condition plays an important role. In this paper, we firstly present a new second-order Toeplitz type approximation to a general hypersingular integral operator. We also give an implementation of the Toeplitz type approximations to the nonlocal integral operators of the cavity model. Negative definiteness of both real and imaginary parts of the discrete matrix for the TE case are proved. Similar results for the TM case were presented in [5]. Secondly, we present second-order finite difference schemes for both the TM and the TE cases. The existence and uniqueness of the finite difference solution for the TE case are established for arbitrary wavenumbers. Fast algorithms for the second-order systems from a rectangular cavity with layered media are obtained. Similar to the fast algorithm proposed in [5], these algorithms also are based on the use of discrete Fourier transform in the horizontal direction and the Gaussian elimination in the vertical direction, by which the global system is reduced to a linear system on the aperture of the cavity. More important is that these algorithms are easy to implement as a preconditioner for cavity models with more general media.

The rest of the paper is organized as follows. In Section 2, the model scattering problem is formulated and further reduced to a bounded domain problem. In Section 3, a new second-order Toeplitz-type scheme is presented for the hypersingular integral operator and the second-order finite difference scheme is employed for the approximation to the governing equations. The existence and uniqueness of the numerical solution for the TE case are proved. The fast algorithm proposed in [5] is extended to solving the linear systems from both TM and TE cases. Several issues on implementation and complexity of

the fast algorithm are addressed. Section 4 is devoted to numerical experiments of the fast algorithm.

2. The electromagnetic scattering from the cavity

We focus on a two-dimensional geometry by assuming that the medium and material are invariant in the z-direction. Assume also that the medium is non-magnetic and a constant magnetic permeability $\mu = \mu_0$ exists everywhere. The electromagnetic property of the medium is characterized by the dielectric coefficient ϵ with $\mathrm{Im}(\epsilon) \geq 0$.

Assume that a plane wave $u^i = e^{\mathrm{i}(\alpha x - \beta y)}$ is the incident wave above the cavity, where $\alpha = k_0 \sin\theta$, $\beta = k_0 \cos\theta$, and $-\pi/2 < \theta < \pi/2$ is the angle of incidence with respect to the positive y-axis. Let u^r be the reflected wave. The relation between the scattered field u^s and the total field u can be expressed by

$$u^s = u - u^i - u^r . \tag{2.1}$$

For the TM (transverse magnetic) polarization, since both the incident electric field and the cavity are independent of the z-axis (that is, no variation with respect to the z-axis), the scattered electric field and the total electric field are also independent of the z-axis. Assuming that $E_z^i = u^i(x,y)$ and $E_z = u(x,y)$, we have $u^r = -e^{\mathrm{i}(\alpha x + \beta y)}$. The time-harmonic Maxwell equations reduce to

$$\Delta u + k^2 u = f(x,y) \qquad (x,y) \in \Omega \cup R_2^+, \tag{2.2}$$

$$u = 0 \qquad \text{on } \Gamma^C \cup (\partial\Omega \setminus \Gamma), \tag{2.3}$$

together with the radiation boundary condition

$$\lim_{r\to\infty} \sqrt{r}\left(\frac{\partial u^s}{\partial r} - \mathrm{i}k_0 u^s\right) = 0, \tag{2.4}$$

where R_2^+ denotes the upper-half space, $r = \sqrt{x^2+y^2}$, $k^2 = \omega^2\epsilon\mu = k_0^2\epsilon_r\mu_r$, $k_0 = \omega\sqrt{\epsilon_0\mu_0}$ is the wavenumber in free space, ω is the angular frequency, $\epsilon_r = \epsilon/\epsilon_0$ and $\mu_r = \mu/\mu_0$ denote the relative permittivity and the relative permeability, respectively. The field is said to be source free if the source term $f(x,y) = 0$.

For the TE (transverse electric) polarization, assuming that $H_z^i = u^i(x,y)$ and $H_z = u(x,y)$, we have $u^r = e^{\mathrm{i}(\alpha x + \beta y)}$. The Maxwell equations reduce to

$$\nabla \cdot \left(\frac{1}{\epsilon_r}\nabla u\right) + k_0^2 \mu_r u = f(x,y) \qquad (x,y) \in \Omega \cup R_2^+, \tag{2.5}$$

$$\frac{\partial u}{\partial n} = 0 \qquad \text{on } \Gamma^C \cup (\partial\Omega \setminus \Gamma),$$

with the same radiation boundary condition (2.4) for the scattered magnetic field. Here, n denotes the unit outward normal.

Since the medium in the upper-half space is homogeneous, a so-called transparent boundary condition can be obtained by using either a Green's function method (*i.e.*, Hankel's function) [8] or a Fourier's transform method [1] for the TM case and the TE case, respectively.

2.1. Formulation for the TM case

In the TM case, the scattered field u^s satisfies

$$\begin{aligned} &\Delta u^s + k_0^2 u^s = 0 \qquad && (x,y) \in R_2^+, \\ &u^s = 0 && \text{on } \Gamma^C, \\ &u^s = u(x,0) && \text{on } \Gamma, \end{aligned}$$

together with the radiation boundary condition (2.4) at infinity.

Let $J_\nu(z)$ and $Y_\nu(z)$ be the ν order Bessel functions of the first kind and the second kind, respectively. The Hankel function $H_\nu^{(1)}(z)$ is defined by

$$H_\nu^{(1)}(z) = J_\nu(z) + \mathrm{i}Y_\nu(z).$$

Let

$$G_d(\boldsymbol{x},\boldsymbol{x}') = \frac{\mathrm{i}}{4}\left[H_0^{(1)}(k_0 r) - H_0^{(1)}(k_0 \bar{r})\right]$$

be the upper half-plane Dirichlet Green's function for the Helmholtz equation, where $\boldsymbol{x} = (x,y)$, $\boldsymbol{x}' = (x',y')$, $r = |\boldsymbol{x} - \boldsymbol{x}'|$, $\bar{r} = |\boldsymbol{x} - \bar{\boldsymbol{x}}'|$ and $\bar{\boldsymbol{x}}' = (x',-y')$ is the image of $\boldsymbol{x}'$ with respect to the real axis. By the Green's theorem and the boundary conditions, we obtain

$$\left.\frac{\partial u^s(\boldsymbol{x})}{\partial y}\right|_{y=0^+} = \frac{\mathrm{i}k_0}{2}\int_\Gamma \left[\frac{1}{|x-x'|}H_1^{(1)}(k_0|x-x'|)u^s(x',0)\right] dx'. \tag{2.6}$$

Substituting (2.1) into (2.6), we have

$$\left.\frac{\partial u}{\partial y}\right|_{y=0^+} = \frac{\mathrm{i}k_0}{2}\int_\Gamma \frac{1}{|x-x'|}H_1^{(1)}(k_0|x-x'|)u(x',0)dx' - 2\mathrm{i}\beta e^{\mathrm{i}\alpha x},\ x \in \Gamma.$$

By the electric field continuity condition

$$\left.\frac{\partial u}{\partial n}\right|_{y=0^+} = \frac{1}{\mu_r}\left.\frac{\partial u}{\partial n}\right|_{y=0^-},$$

and $\mu_r = 1$, the transparent boundary condition for the TM case is given by

$$\frac{\partial u}{\partial n} = I(u) + g(x) \quad x \in \Gamma, \tag{2.7}$$

where $n = (0,1)$, $g(x) = -2\mathrm{i}\beta e^{\mathrm{i}\alpha x}$ and

$$I(u)(x,0) := \frac{\mathrm{i}k_0}{2}\int_\Gamma \frac{1}{|x-x'|}H_1^{(1)}(k_0|x-x'|)u(x',0)dx'. \tag{2.8}$$

Since u satisfies the Helmholtz equation (2.2) and the transparent boundary condition (2.7), the total field u satisfies the following equation

$$\Delta u + k^2 u = f(x,y) \qquad (x,y) \in \Omega, \tag{2.9}$$
$$u = 0 \qquad \text{on } \partial\Omega \setminus \Gamma, \tag{2.10}$$
$$\frac{\partial u}{\partial n} = I(u) + g(x) \qquad \text{on } \Gamma. \tag{2.11}$$

2.2. Formulation for the TE case

Similarly, one can derive the formulation for the TE polarization. In this case, the formulation is different, due to a different type of boundary integral equation.

Let the incident magnetic field take the form $H_z^i = u^i$. Then, the reflected magnetic field $u^r = e^{\mathrm{i}(\alpha x+\beta y)}$, and the scattered magnetic field u^s satisfies

$$\Delta u^s + k_0^2 u^s = 0 \qquad (x,y) \in R_2^+,$$
$$\frac{\partial u^s}{\partial n} = 0 \qquad \text{on } \Gamma^C,$$
$$\frac{\partial u^s}{\partial n} = \frac{\partial u}{\partial n} \qquad \text{on } \Gamma,$$

together with the radiation boundary condition (2.4) at infinity. Let

$$G_n(\boldsymbol{x},\boldsymbol{x}') = \frac{\mathrm{i}}{4}\left[H_0^{(1)}(k_0 r) + H_0^{(1)}(k_0 \bar{r})\right]$$

be the upper half-plane Neumann Green's function for the Helmholtz equation. Following the same procedure as for the TM case, we obtain

$$u^s(\boldsymbol{x}) = -\int_\Gamma \left[G_n(\boldsymbol{x}',\boldsymbol{x})\frac{\partial u^s(\boldsymbol{x}')}{\partial y'}\right]_{y'=0^+} dx'.$$

Substituting (2.1) and (2.2) into the above formula, we obtain

$$u(x) = 2e^{\mathrm{i}\alpha x} - \frac{\mathrm{i}}{2}\int_\Gamma H_0^{(1)}(k_0|x'-x|)\left.\frac{\partial u(\boldsymbol{x}')}{\partial y'}\right|_{y'=0^+} dx'.$$

By the magnetic field continuity condition

$$u(x,y)\big|_{y=0^+} = u(x,y)\big|_{y=0^-} \quad \text{and} \quad \left.\frac{\partial u}{\partial n}\right|_{y=0^+} = \frac{1}{\epsilon_r}\left.\frac{\partial u}{\partial n}\right|_{y=0^-},$$

the transparent boundary condition for the TE case is given by

$$u = \tilde{I}\left(\frac{\partial u}{\partial n}\right) + \tilde{g}(x), \tag{2.12}$$

where $\tilde{g}(x) = 2e^{i\alpha x}$ and

$$\tilde{I}(\frac{\partial u}{\partial n})(x,0) := -\frac{i}{2}\int_\Gamma \frac{1}{\epsilon_r(x')} H_0^{(1)}(k_0|x'-x|)\frac{\partial u(\boldsymbol{x}')}{\partial y'}\bigg|_{y'=0^-} dx'. \quad (2.13)$$

In the TE case, the corresponding Helmholtz-type equation and the transparent boundary condition for the total magnetic field can be written by

$$\nabla\cdot\left(\frac{1}{\epsilon_r}\nabla u\right) + k_0^2\mu_r u = f(x,y) \qquad (x,y)\in\Omega, \quad (2.14)$$

$$\frac{\partial u}{\partial n} = 0 \qquad \text{on } \partial\Omega\setminus\Gamma, \quad (2.15)$$

$$u = \tilde{I}(\frac{\partial u}{\partial n}) + \tilde{g} \qquad \text{on } \Gamma. \quad (2.16)$$

The existence and uniqueness of weak solutions of (2.9)-(2.11) and (2.14)-(2.16) for arbitrary wavenumbers have been obtained in [1]. The proof is based on a variational approach by using the Fredholm alternative along with the fact that the imaginary part of the nonlocal integral operator is nonnegative.

3. Discretization and fast algorithm

Numerical approximations to the cavity model consist of two parts: the approximation to the Helmholtz equation defined in the cavity and the approximation to the nonlocal integral operator on the aperture. In this section, we present a second-order finite difference scheme for the Helmholtz equations and a second-order Toeplitz type approximation to the nonlocal integral operators for the TM and the TE cases, respectively.

3.1. Approximation of nonlocal integral operator

In this subsection, we consider second-order approximations to the nonlocal integral operators (2.8) and (2.13). The nonlocal integral operators (2.8) and (2.13) can be rewritten by

$$I(u)(x,0) = -\frac{k_0}{2}\int_\Gamma \frac{u(x',0)}{|x-x'|}Y_1(k_0|x-x'|)dx' + \frac{ik_0}{2}\int_\Gamma \frac{u(x',0)}{|x-x'|}J_1(k_0|x-x'|)dx', \quad (3.1)$$

and

$$\begin{aligned}\tilde{I}(\frac{\partial u}{\partial n})(x,0) =& \frac{1}{2}\int_\Gamma \frac{1}{\epsilon_r(x')}Y_0(k_0|x'-x|)\frac{\partial u(\boldsymbol{x}')}{\partial y'}\bigg|_{y'=0^-} dx' \\ &- \frac{i}{2}\int_\Gamma \frac{1}{\epsilon_r(x')}J_0(k_0|x'-x|)\frac{\partial u(\boldsymbol{x}')}{\partial y'}\bigg|_{y'=0^-} dx', \end{aligned} \quad (3.2)$$

respectively. Here $\oint\!\!\!\!\!\!-_\Gamma$ denotes a Hadamard finite part (or hypersingular) integral, since

$$Y_1(z) \sim -\frac{2}{\pi z} \quad \text{as} \quad z \to 0\,.$$

The first part of right hand side of (3.2) is a weakly singular integral, since

$$Y_0(z) \sim \frac{2}{\pi} \ln \frac{z}{2} \quad \text{as} \quad z \to 0\,.$$

Other two integral operators in (3.1) and (3.2) are smooth.

Firstly, we consider the nonlocal integral operator (3.1), where the real part is hypersingular and the imaginary part is smooth. Numerical approximation to a hypersingular integral is more complicated than those to a Riemann integral. Quadrature rules for hypersingular integrals have been studied by many authors, see, *e.g.*, [14, 21, 22]. More recently, Wu et al. [23] have provided several Toeplitz or nearly Toeplitz approximations to the following hypersingular integral operator

$$\begin{aligned} Lv(x) &= \oint\!\!\!\!\!\!-_0^1 \frac{v(x')}{(x-x')^2} dx' \\ &= \lim_{\varepsilon \to 0} \left\{ \int_0^{x-\varepsilon} \frac{u(x')}{(x-x')^2} dx' + \int_{x+\varepsilon}^1 \frac{u(x')}{(x-x')^2} dx' - \frac{2u(x)}{\varepsilon} \right\} \end{aligned} \tag{3.3}$$

with $v(0) = v(1) = 0$. Based on a first-order algorithm in [23] (Algorithm II), we propose a new simpler second-order Toeplitz-type approximation to (3.3).

Let $0 = x_0 < x_1 < \cdots < x_n < x_{n+1} = 1$ be a uniform mesh on $[0,1]$ with the mesh size $h = 1/(n+1)$. Denote by

$$v_h^1(x) = \sum_{j=0}^{n+1} v(x_j) \phi_j^1(x)$$

the piecewise polynomial interpolation of $v(x)$, where $\phi_j^1(x)$ are the piecewise linear basis functions, satisfying $\phi_j^1(x_i) = \delta_{ij}$. We introduce a linear operator $\mathscr{K}$ by

$$\begin{aligned} \mathscr{K}v(x) = \lim_{\varepsilon \to 0} \Bigg\{ & \int_0^{x-\varepsilon} \frac{v(x')}{(x'-x)^2} dx' - \frac{v(x^-)}{\varepsilon} - v'(x^-) \ln \varepsilon \\ & + \int_{x+\varepsilon}^1 \frac{v(x')}{(x'-x)^2} dx' - \frac{v(x^+)}{\varepsilon} + v'(x^+) \ln \varepsilon \Bigg\} \end{aligned} \tag{3.4}$$

for $x \in (0,1)$. Actually, if the first derivative of $v(x)$ is Hölder continuous on $[0,1]$, we have that $\mathscr{K}u(x) = Lu(x)$. (See [23])

The new algorithm is defined by

$$\begin{aligned} Lv(x_i) \approx & L_h v(x_i) := \mathcal{K} v_h^1(x_i) + \frac{v(x_{i-1}) - 2v(x_i) + v(x_{i-1})}{h^2}(h - \ln h) \\ & + \sum_{j=1}^{i-1} \frac{v(x_{j-1}) - 2v(x_j) + v(x_{j+1})}{h^2} \int_{x_{j-1}}^{x_j} \frac{(x' - x_{j-1})(x' - x_j)}{2(x' - x_i)^2} dx' \\ & + \sum_{j=i+1}^{n} \frac{v(x_{j-1}) - 2v(x_j) + v(x_{j+1})}{h^2} \int_{x_j}^{x_{j+1}} \frac{(x' - x_j)(x' - x_{j+1})}{2(x' - x_i)^2} dx' \\ := & \sum_{j=1}^{n} \alpha_{ij} v_j. \end{aligned} \tag{3.5}$$

A straightforward calculation gives

$$\alpha_{ij} = \delta_{1j} c_{i1} + \delta_{jn} c_{i2} + \begin{cases} -(2 + 3\ln 2)/h, & i = j, \\ (1 + \frac{9}{2}\ln 2 - \frac{5}{2}\ln 3)/h, & |i - j| = 1, \\ [(3s_{ij} + \frac{3}{2})\ln(s_{ij} + 1) + (\frac{3}{2} - 3s_{ij})\ln s_{ij} & \\ \quad -(s_{ij} + \frac{3}{2})\ln(s_{ij} + 2) + (s_{ij} - \frac{3}{2})\ln(s_{ij} - 1)]/h, & \text{others}, \end{cases} \tag{3.6}$$

where

$$c_{i1} = -\left(1 + (i + \frac{1}{2})\ln\frac{i}{i+1}\right), \quad c_{i2} = c_{n-i+1,1}, \quad s_{ij} = |i - j|. \tag{3.7}$$

Obviously, the matrix (α_{ij}) is a Toeplitz matrix plus a matrix with only two nonzero columns.

Theorem 3.1. *Let $L_h v(x_i)$ be defined by* (3.5). *Then for $v(x) \in C^3[a, b]$, it holds that*

$$|Lv(x_i) - L_h v(x_i)| \le Ch^2, \quad 1 \le i \le n. \tag{3.8}$$

Proof. It follows from the proof of Theorem 2.1 of [23] that

$$Lv(x_i) = \mathcal{K} v_h^1(x_i) + \frac{2v(x_i) - v(x_{i+1}) - v(x_{i-1})}{h^2} \ln h + \mathcal{I}_1 + \mathcal{I}_2 + \mathcal{I}_3,$$

where

$$\begin{aligned} \mathcal{I}_1 &= \int_0^{x_{i-1}} \frac{e_1(x')}{(x' - x_i)^2} dx', \quad \mathcal{I}_2 = \int_{x_{i+1}}^1 \frac{e_1(x')}{(x' - x_i)^2} dx', \\ \mathcal{I}_3 &= \left(\int_{x_{i-1}}^{x_i} + \int_{x_i}^{x_{i+1}}\right) \frac{v(x') - v(x_i) - v'(x_i)(x' - x_i)}{(x' - x_i)^2} dx' \end{aligned}$$

and $e_1(x) = v(x) - v_h^1(x)$. Since $v(x) \in C^3[0, 1]$,

$$e_1(x') = \frac{v''(x_j)}{2}(x' - x_j)(x' - x_{j+1}) + \mathcal{O}(h^3), \quad x' \in (x_j, x_{j+1}).$$

Approximating $v''(x')$ by the central finite difference

$$v''(x_i)=\frac{v(x_{i-1})-2v(x_i)+v(x_{i+1})}{h^2}+\mathcal{O}(h^2)$$

in the above equation, we obtain

$$\mathscr{I}_1=\sum_{j=1}^{i-1}\frac{v(x_{j-1})-2v(x_j)+v(x_{j+1})}{h^2}\int_{x_{j-1}}^{x_j}\frac{(x'-x_{j-1})(x'-x_j)}{2(x'-x_i)^2}dx'+\mathcal{O}(h^2),$$
$$\mathscr{I}_2=\sum_{j=i+1}^{n}\frac{v(x_{j-1})-2v(x_j)+v(x_{j+1})}{h^2}\int_{x_j}^{x_{j+1}}\frac{(x'-x_j)(x'-x_{j+1})}{2(x'-x_i)^2}dx'+\mathcal{O}(h^2),$$
$$\mathscr{I}_3=\frac{v(x_{i-1})-2v(x_i)+v(x_{i+1})}{h}+\mathcal{O}(h^2).$$

The error estimate (3.8) follows immediately. □

To apply the above algorithm for the real part of the nonlocal integral operator (3.1), we rewrite the real part by

$$\mathrm{Re}(I(u)(x,0))=-\frac{1}{2}=\!\!\!\!\!\!\int_\Gamma\frac{1}{(x-x')^2}\widetilde{Y}_1(k_0|x-x'|)u(x',0)dx',$$

where $\widetilde{Y}_1(z)=zY_1(z)$. A second-order approximation to the above integral operator is defined by

$$\mathrm{Re}(I(u)(x_i,0))\approx-\frac{1}{2}\sum_{j=1}^{M}\alpha_{ij}\widetilde{Y}_1(k_0|x_i-x_j|)u(x_j,0):=\sum_{j=1}^{M}g_{ij}^{\mathrm{re}}u(x_j,0),\tag{3.9}$$

where $g_{ij}^{\mathrm{re}}=-\alpha_{ij}\widetilde{Y}_1(k_0|x_i-x_j|)/2$ and α_{ij} is defined in (3.6).

Since the imaginary part of (3.1) is smooth, we use the classical trapezoidal rule. Then, the discrete scheme for the imaginary part is given by

$$\mathrm{Im}(I(u)(x_i,0))\approx\frac{k_0^2}{2}\int_\Gamma\widetilde{J}_1(k_0|x_i-x'|)u(x',0)dx':=\sum_{j=1}^{M}g_{ij}^{\mathrm{im}}u(x_j,0),$$

where

$$\widetilde{J}_1(z):=J_1(z)/z,\quad g_{ij}^{\mathrm{im}}=\frac{k_0^2h}{2}\tilde{J}_1(k_0|x_i-x_j|).$$

In terms of those basic results in numerical integration, we see that the above approximations have a second-order accuracy.

We denote the discrete nonlocal operator for the TM case by

$$G=G^{\mathrm{re}}+\mathrm{i}G^{\mathrm{im}}$$

with $G^{\mathrm{re}}=\left(g_{ij}^{\mathrm{re}}\right)$ and $G^{\mathrm{im}}=\left(g_{ij}^{\mathrm{im}}\right)$. G is a Toeplitz matrix plus a matrix with only two nonzero columns. The classical fast algorithm can be applied for the matrix-vector multiplication [6,8].

Theorem 3.2 ([5]). *The matrix* $G^{\mathrm{im}} = \left(g_{ij}^{\mathrm{im}}\right)$ *in* (3.10) *is symmetric positive definite.*

Secondly, we consider the nonlocal integral operator (3.2) for the TE case, which can be rewritten by

$$\tilde{I}(v)(x) = \frac{1}{2}\int_{\Gamma} \frac{1}{\epsilon_r(x')} Y_0(k_0|x-x'|)v(x')dx' - \frac{\mathrm{i}}{2}\int_{\Gamma} \frac{1}{\epsilon_r(x')} J_0(k_0|x-x'|)v(x')dx'. \quad (3.10)$$

Since the first part in (3.10) is weakly singular and the second part is smooth, we use a piecewise linear approximation to the first part and the classical trapezoidal rule for the second part. A general approximation for the integral operator (3.10) is written by

$$\tilde{I}(v)(x_i) \approx \sum_{j=1}^{M} t_{ij} \frac{v_j}{\epsilon_r(x_j)}, \quad (3.11)$$

where $t_{ij} = t_{ij}^{\mathrm{re}} + \mathrm{i}t_{ij}^{\mathrm{im}}$ and

$$t_{ij}^{\mathrm{re}} = \frac{1}{2}\int_{\Gamma} Y_0(k_0|x_i - x'|)\phi_j^1(x')dx', \quad (3.12)$$

$$t_{ij}^{\mathrm{im}} = -\frac{h_x}{2} J_0(k_0|x_i - x_j|). \quad (3.13)$$

Obviously, the above approximation gives a second-order accuracy.

Theorem 3.3. *Let* $T = T^{\mathrm{re}} + \mathrm{i}T^{\mathrm{im}}$ *with* $T^{\mathrm{re}} = \left(t_{ij}^{\mathrm{re}}\right)$ *and* $T^{\mathrm{im}} = \left(t_{ij}^{\mathrm{im}}\right)$ *being defined by* (3.12) *and* (3.13)*, respectively. Then the matrices* T^{re} *and* T^{im} *are symmetric negative definite and the matrix* T *is nonsingular symmetric Toeplitz.*

Proof. Firstly, we consider the matrix T^{im}. According to the definition of T^{im}, it is obvious that T^{im} is symmetric Toeplitz matrix. Since

$$J_0(z) = \frac{1}{\pi}\int_{-1}^{1} (1-t^2)^{-1/2} e^{\mathrm{i}zt} dt,$$

we have

$$t_{lj}^{\mathrm{im}} = -\frac{h_x}{2\pi}\int_{-1}^{1} (1-t^2)^{-1/2} e^{\mathrm{i}k_0|x_l - x_j|t} dt.$$

Let $v = (v_1, v_2, \cdots, v_N)^T$ be a real vector. We obtain

$$v^T T^{\mathrm{im}} v = -\frac{h_x}{2\pi}\sum_{l=1}^{M}\sum_{j=1}^{M} v_l v_j \int_{-1}^{1} (1-t^2)^{-1/2} \cos(k_0(x_l - x_j)t) dt.$$

By a straightforward calculation, we have

$$\begin{aligned} v^T T^{\mathrm{im}} v &= -\frac{h_x}{2\pi}\int_0^1 \frac{1}{\sqrt{1-t^2}}\sum_{l=1}^{M}\sum_{j=1}^{M}\left(e^{\mathrm{i}k_0(l-j)th_x}+e^{-\mathrm{i}k_0(l-j)th_x}\right)v_l v_j dt \\ &= -\frac{h_x}{2\pi}\int_0^1 \frac{1}{\sqrt{1-t^2}}\left(\left|\sum_{j=1}^{M} e^{-\mathrm{i}k_0 tjh_x}v_j\right|^2+\left|\sum_{l=1}^{M} e^{\mathrm{i}k_0 tlh_x}v_l\right|^2\right)dt \le 0\,. \end{aligned}$$

If $v^T T^{\mathrm{im}} v = 0$, we get

$$\sum_{j=1}^{M} e^{-\mathrm{i}k_0 tjh_x}v_j = 0, \quad \text{and} \quad \sum_{l=1}^{M} e^{\mathrm{i}k_0 tlh_x}v_l = 0,$$

which lead to $v = 0$. Thus, T^{im} is symmetric negative definite.

Secondly, we consider the matrix T^{re}. By the classical formula

$$Y_0(z) = -\frac{2}{\pi}\int_1^{\infty}\frac{\cos(zt)}{\sqrt{(t^2-1)}}dt,$$

we have

$$\begin{aligned} t_{lj}^{\mathrm{re}} &= -\frac{1}{\pi}\int_\Gamma\left(\int_1^{\infty}\frac{\cos(k_0|x_l-x'|t)}{\sqrt{(t^2-1)}}dt\right)\phi_j^1(x')dx' \\ &= -\frac{1}{\pi}\int_1^{\infty}\frac{1}{\sqrt{(t^2-1)}}\left(\int_0^a \cos(k_0(x_l-x')t)\phi_j^1(x')dx'\right)dt\,. \end{aligned}$$

A straightforward calculation gives

$$\int_0^a \cos(k_0(x_l-x')t)\phi_j^1(x')dx' = \frac{2(1-\cos(k_0 th_x))\cos((l-j)k_0 th_x)}{t^2k_0^2h_x}$$

and therefore,

$$t_{lj}^{\mathrm{re}} = -\frac{2}{\pi k_0^2 h_x}\int_1^{\infty}\eta(t)\cos((l-j)k_0 th_x)dt,$$

where

$$\eta(t) = \frac{(1-\cos(k_0 th_x))}{t^2\sqrt{(t^2-1)}}.$$

It follows that T^{re} is a symmetric Toeplitz matrix and moreover,

$$\begin{aligned} v^T T^{\mathrm{re}} v &= \sum_{l=1}^{M}\sum_{j=1}^{M} t_{lj}^{\mathrm{re}} v_l v_j \\ &= -\frac{2}{\pi k_0^2 h_x}\sum_{l=1}^{M}\sum_{j=1}^{M} v_l v_j \int_1^{\infty} \eta(t)\cos((l-j)k_0 t h_x)dt \\ &= -\frac{2}{\pi k_0^2 h_x}\int_1^{\infty} \eta(t)\left(\left|\sum_{l=1}^{M} e^{\mathrm{i}k_0 t l h_x} v_l\right|^2 + \left|\sum_{j=1}^{M} e^{-\mathrm{i}k_0 t j h_x} v_j\right|^2\right) dt \le 0, \end{aligned}$$

which shows that the matrix T^{re} also is symmetric negative definite.

Finally, we see that the matrix T is nonsingular since the matrices T^{re} and T^{im} are symmetric negative definite. □

3.2. TM case

Bao and Sun [5] presented a first-order scheme, in which a first-order approximation was used for the transparent boundary condition and a second-order approximation was used for the Helmholtz equation. If we use a second-order approximation to the transparent boundary condition, we may obtain a second-order method. Let $\{x_i, y_j\}_{i,j=0}^{M+1,N+1}$ define a uniform partition of $\Omega = [0,a]\times[-b,0]$ with $x_{i+1}-x_i = h_x$ and $y_{j+1}-y_j = h_y$. Let u_{ij} be the finite difference solution at the point (x_i, y_j). The discrete finite difference system for the TM case can be given by

$$\begin{aligned} &\frac{u_{i-1,j}-2u_{ij}+u_{i+1,j}}{h_x^2} + \frac{u_{i,j-1}-2u_{ij}+u_{i,j+1}}{h_y^2} + k^2(x_i,y_j)u_{ij} = f(x_i,y_j), \quad (3.14)\\ &u_{0j} = u_{M+1,j} = u_{i0} = 0, \quad i = 1,\cdots,M, \quad j = 1,\cdots,N+1. \end{aligned}$$

Note that the fictitious points (x_i, y_{N+2}) are used in the system (3.14) [15]. The solution at these points will be eliminated by the use of the following second-order approximation of the transparent boundary condition

$$\frac{u_{i,N+2}-u_{iN}}{2h_y} = \sum_{l=1}^{M} g_{il}u_{l,N+1} + g(x_i), \quad i = 1,\cdots,M, \tag{3.15}$$

which can be rewritten by

$$\frac{u_{i,N+2}-u_{iN}}{h_y^2} = \frac{2}{h_y}Gu_{:,N+1} + \frac{2}{h_y}g, \quad i = 1,\cdots,M, \tag{3.16}$$

where $G = (g_{ij})_{i,j=1}^{M}$ is defined in (3.9)-(3.10). It is easy to show that the truncation error of above approximation is $\mathcal{O}(h_x^2 + h_y^2)$ when the solution is smooth.

If the medium inside the cavity is horizontally homogeneous, the equations at the interior of cavity in (3.14) can be rewritten by

$$\left(A_x \otimes I_N + I_M \otimes (A_y + D_L)\right) U_1 + (I_M \otimes a_{N+1}) u_{:,N+1} = F_1, \tag{3.17}$$

where I_M is the $M \times M$ identity matrix,

$$A_x = \frac{1}{h_x^2}\begin{pmatrix} -2 & 1 & & & \\ 1 & -2 & 1 & & \\ & \ddots & \ddots & \ddots & \\ & & & 1 & -2 \end{pmatrix}, \quad A_y = \frac{1}{h_y^2}\begin{pmatrix} -2 & 1 & & & \\ 1 & -2 & 1 & & \\ & \ddots & \ddots & \ddots & \\ & & & 1 & -2 \end{pmatrix},$$

$$D_L = \operatorname{diag}\left(k^2(y_1), k^2(y_2), \cdots, k^2(y_N)\right), \quad a_{N+1} = \frac{1}{h_y^2}(0, \cdots, 0, 1)^T,$$

$$U_1 = (u_{11}, u_{12}, \cdots, u_{1N}, u_{21}, u_{22}, \cdots, u_{2N}, \cdots, u_{M1}, \cdots, u_{MN})^T,$$

$$F_1 = (f_{11}, f_{12}, \cdots, f_{1N}, f_{21}, f_{22}, \cdots, f_{2N}, \cdots, f_{M1}, \cdots, f_{MN})^T,$$

$$u_{:,j} = (u_{1j}, u_{2j}, \cdots, u_{Mj})^T,$$

and $\otimes$ denotes the tensor product (Kronecker product). We extend a fast algorithm proposed by [5] to the system in (3.14)-(3.15) below. For the tridiagonal Toeplitz matrix A_x, we have

$$S_M A_x S_M = \Lambda = \operatorname{diag}\left(\lambda_1, \lambda_2, \cdots, \lambda_M\right),$$

where S_M denotes the discrete Fourier-sine transform,

$$S_M = \sqrt{\frac{2}{M+1}}\left(\sin\frac{lm\pi}{M+1}\right)_{l,m=1}^{M}, \qquad \lambda_l = -\frac{4(M+1)^2}{a^2}\sin^2\frac{l\pi}{2(M+1)},$$

and $S_M^2 = I$. By the discrete Fourier-sine transform, we rewrite (3.17) by

$$\left(\Lambda \otimes I_N + I_M \otimes (A_y + D_L)\right) \bar{U}_1 + (I_M \otimes a_{N+1}) \bar{u}_{:,N+1} = \bar{F}_1, \tag{3.18}$$

where

$$\bar{U}_1 = \left(S_M \otimes I_N\right) U_1 = (\bar{u}_{11}, \cdots, \bar{u}_{1N}, \bar{u}_{21}, \cdots, \bar{u}_{2N}, \cdots, \bar{u}_{M1}, \cdots, \bar{u}_{MN})^T,$$
$$\bar{F}_1 = \left(S_M \otimes I_N\right) F_1 = (\bar{f}_{11}, \cdots, \bar{f}_{1N}, \bar{f}_{21}, \cdots, \bar{f}_{2N}, \cdots, \bar{f}_{M1}, \cdots, \bar{f}_{MN},)^T,$$
$$\bar{u}_{:,j} = S_M u_{:,j} = (\bar{u}_{1j}, \bar{u}_{2j}, \cdots, \bar{u}_{Mj})^T.$$

Reordering the unknowns and equations in (3.18), we obtain

$$(A_y + \lambda_i I_N + D_L)\bar{u}_{i,:} + a_{N+1}\bar{u}_{i,N+1} = \bar{f}_{i,:}, \qquad i = 1, \cdots, M, \tag{3.19}$$

where

$$\bar{u}_{i,:} = (\bar{u}_{i1}, \bar{u}_{i2}, \cdots, \bar{u}_{iN})^T, \quad \bar{f}_{i,:} = (\bar{f}_{i1}, \bar{f}_{i2}, \cdots, \bar{f}_{iN})^T, \quad i = 1, \cdots, M.$$

We use the forward Gaussian elimination method with a row partial pivoting for each system in (3.19) to get M upper Hessenberg systems, in which the last equations are written by

$$\alpha_i \bar{u}_{iN} + \beta_i \bar{u}_{i,N+1} = \hat{f}_{i,N}, \quad i = 1, \cdots, M,$$

or equivalently

$$D_\alpha \bar{u}_{:,N} + D_\beta \bar{u}_{:,N+1} = \hat{f}_{:,N}, \tag{3.20}$$

where

$$D_\alpha = \mathrm{diag}(\alpha_1, \alpha_2, \cdots, \alpha_M), \quad D_\beta = \mathrm{diag}(\beta_1, \beta_2, \cdots, \beta_M).$$

(3.20) also defines a discrete Dirichlet-to-Neumann map. By the discrete Fourier-sine transform, the system (3.16) becomes

$$\begin{aligned} &\frac{1}{h_y^2}\bar{u}_{:,N} + \left(S_M(\frac{1}{2}A_x + \frac{1}{2}D_0 + \frac{1}{h_y}G)S_M - \frac{1}{h_y^2}I_M \right) \bar{u}_{:,N+1} \\ &= \frac{1}{2}S_M f_{:,N+1} - \frac{1}{h_y}S_M g\,. \end{aligned} \tag{3.21}$$

Eliminating $\bar{u}_{:,N}$ from Eq. (3.21) by Eq. (3.20) leads to a system on the interface Γ

$$\begin{aligned} &\left(S_M(\frac{1}{2}A_x + \frac{1}{2}D_0 + \frac{1}{h_y}G)S_M - \frac{1}{h_y^2}(I_M + D_\alpha^{-1}D_\beta) \right) \bar{u}_{:,N+1} \\ &= \frac{1}{2}S_M f_{:,N+1} - \frac{1}{h_y}S_M g - \frac{1}{h_y^2}D_\alpha^{-1}\hat{f}_{:,N}\,. \end{aligned} \tag{3.22}$$

Solving the linear system (3.22) gives the solution $\bar{u}_{:,N+1}$ on the interface Γ. The rest unknowns can be obtained by solving the following systems

$$(A_y + \lambda_i I_N + D_L)\bar{u}_{i,:} = \bar{f}_{i,:} - a_{N+1}\bar{u}_{i,N+1}, \qquad i = 1, \cdots, M, \tag{3.23}$$

where

$$u_{:,N} = \frac{h_y^2}{2}f_{:,N+1} - h_y g - h_y^2(\frac{1}{2}A_x + \frac{1}{2}D_0 + \frac{1}{h_y}G - \frac{1}{h_y^2}I_M)u_{:,N+1}$$

may be used for those possible nearly singular systems. The fast algorithm is given below.

Algorithm I:
(i) Generate the matrix G.
(ii) Calculate the D_α and D_β, by using the forward Gaussian elimination with a row partial pivoting.
(iii) Calculate $\bar{F}_1 = (S_M \otimes I)F_1$, $S_M(\frac{1}{2}f_{:,N+1} - \frac{1}{h_y}g)$ and $D_\alpha^{-1}\hat{f}_{:,N}$.
(iv) Solve the system (3.22) for $\bar{u}_{:,N+1}$.
(v) Solve the system (3.23) for the rest of the unknowns.

3.3. TE case

In this subsection, we study the discretization of Helmholtz equation (2.14) and boundary conditions (2.15)-(2.16) in the TE case. Here, we use an offset grid, i.e., a grid where the boundary points fall halfway between the grid points instead of on the grid points. Let $\{(x_i,y_j): x_i=(i-1)h_x+h_x/2, i=0,1,\cdots,M+1,\ y_j=-b+(j-1)h_y+h_y/2, j=0,1,\cdots,N+1\}$ be a partition of $\Omega=[0,a]\times[-b,0]$, where $h_x=a/M$ and $h_y=b/N$. Note that there are no grid points on the boundaries of the region and the points associated with $i=0$, $i=M+1$, $j=0$ and $j=N+1$ are fictitious points outside of $[0,a]\times[-b,0]$. A discrete finite difference system for Eq. (2.14) can be given by

$$\begin{aligned}&\frac{1}{h_x}\left(\frac{1}{\epsilon_r(x_{i+1/2},y_j)}\frac{u_{i+1,j}-u_{ij}}{h_x}-\frac{1}{\epsilon_r(x_{i-1/2},y_j)}\frac{u_{ij}-u_{i-1,j}}{h_x}\right)\\&+\frac{1}{h_y}\left(\frac{1}{\epsilon_r(x_i,y_{j+1/2})}\frac{u_{i,j+1}-u_{ij}}{h_y}-\frac{1}{\epsilon_r(x_i,y_{j-1/2})}\frac{u_{ij}-u_{i,j-1}}{h_y}\right)\\&+k_0^2(x_i,y_j)\mu_r u_{ij}=f(x_i,y_j),\quad i=1,\cdots,M,\quad j=1,\cdots,N.\end{aligned}\tag{3.24}$$

Using a central finite difference approximation for the derivatives at the boundary, the approximations for the boundary conditions (2.15)-(2.16) are as follows

$$\begin{aligned}&\frac{u_{1j}-u_{0j}}{h_x}=0,\quad j=1,\cdots,N,\\&\frac{u_{M+1,j}-u_{M,j}}{h_x}=0,\quad j=1,\cdots,N,\\&\frac{u_{i1}-u_{i0}}{h_y}=0,\quad i=1,\cdots,M,\end{aligned}\tag{3.25}$$

and

$$\frac{u_{i,N+1}+u_{i,N}}{2}=\frac{1}{h_y}\sum_{l=1}^{M}\frac{1}{\epsilon_r(x_l,y_{N+\frac{1}{2}})}t_{il}(u_{l,N+1}-u_{lN})+\tilde{g}(x_i),\quad i=1,\cdots,M,$$

or equivalently,

$$\left(\frac{1}{2}I_M+\frac{1}{h_y}TD_{\epsilon_r}\right)u_{:,N}+(\frac{1}{2}I_M-\frac{1}{h_y}TD_{\epsilon_r})u_{:,N+1}=\tilde{g},\tag{3.26}$$

where $T=(t_{il})_{i,l=1}^{M}$ is a symmetric nonsingular $M\times M$ matrix defined in (3.12)-(3.13) and

$$D_{\epsilon_r}=\text{diag}\left(\frac{1}{\epsilon_r(x_1,y_{N+\frac{1}{2}})},\frac{1}{\epsilon_r(x_2,y_{N+\frac{1}{2}})},\cdots,\frac{1}{\epsilon_r(x_M,y_{N+\frac{1}{2}})}\right).$$

It is also easy to show that the truncation error of the above approximation is $\mathcal{O}(h_x^2+h_y^2)$ when u and $\epsilon_r(x,y)$ are smooth.

Theorem 3.4. *For any wavenumber k with* $\mathrm{Im}(\epsilon_r(x,y)) \geq 0$*, the system* (3.24)-(3.26) *has a unique solution.*

Proof. Define

$$\varphi_i := \frac{1}{\epsilon_r(x_i, y_{N+\frac{1}{2}})} \frac{u_{i,N+1} - u_{iN}}{h_y}, \quad i = 1, \cdots, M.$$

We can rewrite the equations in (3.24) for $j = N$ by

$$\begin{aligned} &\frac{1}{h_x}\left(\frac{1}{\epsilon_r(x_{i+1/2}, y_N)}\frac{u_{i+1,N} - u_{iN}}{h_x} - \frac{1}{\epsilon_r(x_{i-1/2}, y_N)}\frac{u_{iN} - u_{i-1,N}}{h_x}\right) \\ &+ \frac{1}{h_y}\left(-\frac{1}{\epsilon_r(x_i, y_{N-1/2})}\frac{u_{iN} - u_{i,N-1}}{h_y}\right) + k_0^2(x_i, y_N)\mu_r u_{iN} + \frac{1}{h_y}\varphi_i = f(x_i, y_N) \end{aligned} \tag{3.27}$$

and the transparent boundary condition by

$$\frac{1}{h_y}u_{iN} + \frac{1}{2}\epsilon_r(x_i, y_{N+\frac{1}{2}})\varphi_i - \frac{1}{h_y}\sum_{l=1}^{M} t_{il}\varphi_l = \frac{1}{h_y}\tilde{g}(x_i), \quad i = 1, \cdots, M, \tag{3.28}$$

To prove the uniqueness and existence of the numerical solution, it suffices to prove that the system in (3.24)-(3.26) has only the zero solution when $F = 0$.

From (3.24), (3.27) and (3.28), we obtain

$$\begin{aligned} &\sum_{i=1}^{M}\sum_{j=1}^{N-1} u_{ij}^*\left[\frac{1}{h_x}\left(\frac{1}{\epsilon_r(x_{i+1/2}, y_j)}\frac{u_{i+1,j} - u_{ij}}{h_x} - \frac{1}{\epsilon_r(x_{i-1/2}, y_j)}\frac{u_{ij} - u_{i-1,j}}{h_x}\right)\right. \\ &\left.+\frac{1}{h_y}\left(\frac{1}{\epsilon_r(x_i, y_{j+1/2})}\frac{u_{i,j+1} - u_{ij}}{h_y} - \frac{1}{\epsilon_r(x_i, y_{j-1/2})}\frac{u_{ij} - u_{i,j-1}}{h_y}\right)\right] \\ &+\sum_{i=1}^{M}\sum_{j=1}^{N-1} k_0^2(x_i, y_j)\mu_r u_{ij}^* u_{ij} + \sum_{i=1}^{M} u_{iN}^*\left[\frac{1}{h_x}\left(\frac{1}{\epsilon_r(x_{i+1/2}, y_N)}\frac{u_{i+1,N} - u_{iN}}{h_x}\right.\right. \\ &\left.\left.-\frac{1}{\epsilon_r(x_{i-1/2}, y_N)}\frac{u_{iN} - u_{i-1,N}}{h_x}\right) - \frac{1}{h_y}\left(\frac{1}{\epsilon_r(x_i, y_{N-1/2})}\frac{u_{iN} - u_{i,N-1}}{h_y}\right)\right] \\ &+\sum_{i=1}^{M} k_0^2(x_i, y_N)\mu_r u_{iN}^* u_{iN} + \sum_{i=1}^{M}\frac{1}{h_y}u_{iN}^*\varphi_i = 0 \end{aligned} \tag{3.29}$$

and

$$\frac{1}{h_y}\sum_{i=1}^{M}\varphi_i^* u_{iN} + \frac{1}{2}\sum_{i=1}^{M}\varphi_i^*\epsilon_r(x_i, y_{N+\frac{1}{2}})\varphi_i - \frac{1}{h_y}\sum_{i=1}^{M}\sum_{l=1}^{M}\varphi_i^* t_{il}\varphi_l = 0, \tag{3.30}$$

where the superscript $*$ denotes the conjugate. By the boundary condition (3.25), Eq. (3.29) becomes

$$-\sum_{i=1}^{M}\sum_{j=1}^{N}\frac{1}{\epsilon_r(x_{i+1/2},y_j)}\left|\frac{u_{i+1,j}-u_{ij}}{h_x}\right|^2-\sum_{i=1}^{M}\sum_{j=1}^{N-1}\frac{1}{\epsilon_r(x_i,y_{j+1/2})}\left|\frac{u_{i,j+1}-u_{ij}}{h_y}\right|^2$$
$$+\sum_{i=1}^{M}\sum_{j=1}^{N}k_0^2(x_i,y_j)\mu_r|u_{ij}|^2+\frac{1}{h_y}\sum_{i=1}^{M}u_{iN}^*\varphi_i=0.$$

Moreover, by (3.30), we have

$$-\sum_{i=1}^{M}\sum_{j=1}^{N}\frac{1}{\epsilon_r(x_{i+1/2},y_j)}\left|\frac{u_{i+1,j}-u_{ij}}{h_x}\right|^2-\sum_{i=1}^{M}\sum_{j=1}^{N-1}\frac{1}{\epsilon_r(x_i,y_{j+1/2})}\left|\frac{u_{i,j+1}-u_{ij}}{h_y}\right|^2$$
$$+\sum_{i=1}^{M}\sum_{j=1}^{N}k_0^2(x_i,y_j)\mu_r|u_{ij}|^2+\frac{1}{h_y}\sum_{i=1}^{M}\sum_{l=1}^{M}t_{li}^*\varphi_l^*\varphi_i-\frac{1}{2}\sum_{i=1}^{M}|\varphi_i|^2\epsilon_r^*(x_i,y_{N+1/2})=0.$$

From the imaginary part of the above equation,

$$-\sum_{i=1}^{M}\sum_{j=1}^{N}\mathrm{Im}\left(\frac{1}{\epsilon_r(x_{i+1/2},y_j)}\right)\left|\frac{u_{i+1,j}-u_{ij}}{h_x}\right|^2-\sum_{i=1}^{M}\sum_{j=1}^{N-1}\mathrm{Im}\left(\frac{1}{\epsilon_r(x_i,y_{j+1/2})}\right)\left|\frac{u_{i,j+1}-u_{ij}}{h_y}\right|^2$$
$$+\frac{1}{h_y}\sum_{i=1}^{M}\sum_{l=1}^{M}\mathrm{Im}(t_{li}^*\varphi_l^*\varphi_i)-\frac{1}{2}\sum_{i=1}^{M}|\varphi_i|^2\mathrm{Im}(\epsilon_r^*(x_i,y_{N+1/2}))=0\,.$$

Since $\mathrm{Im}(\epsilon_r(x,y))\geq 0$ and $\mathrm{Im}(1/\epsilon_r(x_i,y_{N+1/2}))\leq 0$, we have

$$\sum_{i=1}^{M}\sum_{l=1}^{N}\mathrm{Im}(t_{li}^*\varphi_l^*\varphi_i)=0\,.$$

By Theorem 3.3, T^{im} and T^{re} are symmetric negative definite. Thus, we have $\varphi_i=0$. It follows from (3.28) that $u_{iN}=0$. Furthermore, from (3.24), we get $u_{ij}=0$. The proof is complete. □

For a cavity filled with horizontally homogeneous media, Eqs. (2.14)-(2.16) for the TE case can be rewritten by

$$\frac{1}{\epsilon_r(y)}\frac{\partial^2 u}{\partial x^2}+\frac{\partial}{\partial y}\left(\frac{1}{\epsilon_r(y)}\frac{\partial u}{\partial y}\right)+k_0^2\mu_r u=f(x,y),\qquad (x,y)\in\Omega,\tag{3.31}$$
$$\frac{\partial u}{\partial n}=0,\qquad \text{on } \partial\Omega\setminus\Gamma,\tag{3.32}$$
$$u=\tilde{I}(\frac{\partial u}{\partial n})+\tilde{g},\qquad \text{on } \Gamma\,.$$

The discrete system defined in (3.24)-(3.26) reduces to

$$\left(A_x^N \otimes B_N + I_M \otimes A_y^{ND} + k_0^2 \mu_r I\right) U_1 + (I_M \otimes E_N) u_{:,N+1} = F_1, \tag{3.33}$$

where

$$A_x^N = \frac{1}{h_x^2}\begin{pmatrix} -1 & 1 & & & \\ 1 & -2 & 1 & & \\ & \ddots & \ddots & \ddots & \\ & & & 1 & -1 \end{pmatrix}, \quad E_N = \frac{1}{h_y^2 \epsilon_r(y_{N+\frac{1}{2}})}\begin{pmatrix} 0 \\ \vdots \\ 0 \\ 1 \end{pmatrix},$$

$$A_y^{ND} = \frac{1}{h_y^2}\begin{pmatrix} -\epsilon_{r,+}^{(1)}, & \epsilon_{r,+}^{(1)} & & \\ \epsilon_{r,-}^{(2)}, & -\left(\epsilon_{r,-}^{(2)} + \epsilon_{r,+}^{(2)}\right), & \epsilon_{r,+}^{(2)} & \\ & \ddots & \ddots & \ddots \\ & & \epsilon_{r,-}^{(N)}, & -\left(\epsilon_{r,-}^{(N)} + \epsilon_{r,+}^{(N)}\right) \end{pmatrix},$$

$$B_N = \operatorname{diag}\left(\frac{1}{\epsilon_r(y_1)}, \frac{1}{\epsilon_r(y_2)}, \cdots, \frac{1}{\epsilon_r(y_N)}\right),$$

where $\epsilon_{r,\pm}^{(j)} = 1/\epsilon_r(y_{j\pm 1/2})$.

A fast algorithm for the TE case can be designed analogously by replacing A_x and A_y in the Fast Algorithm I with A_x^N and A_y^{ND}.

3.4. Implementation, complexity and preconditioning

Table 1: The real arithmetic operation counts of the fast algorithm.

Step	Calculate U with $f \neq 0$	Calculate $u_{:,N+1}$ with $f = 0$
Step (i)	$\mathcal{O}(M)$	$\mathcal{O}(M)$
Step (ii)	$5MN$	$3MN$
Step (iii)	$2NM \log M$	$2M \log M$
Step (iv)	$\mathcal{O}(12pM \log M)$	$\mathcal{O}(12pM \log M)$
Step (v)	$\mathcal{O}(NM \log M)$	0
Total	$\mathcal{O}(NM \log M + 12pM \log M)$	$\mathcal{O}(MN + 12pM \log M)$

According to the discussion in Subsection 3.1, the cost of Step (i) in the Algorithm I is $\mathcal{O}(M)$. The costs for other steps are very similar to those presented in [5]. We summarize in Table 1 the cost (real arithmetic operations) for each step, where p is the number of iterations used for solving the system (3.22). When $f(x,y) \neq 0$, the cost of the algorithm is $\mathcal{O}(NM \log M)$ if p is not large. More importantly, in the source free case, the cost decreases significantly to $\mathcal{O}(MN)$ for an $M \times N$ mesh if $p \leq N/\log M$, which will be illustrated numerically in the next section.

The key to the fast algorithm is the iterative solver for the interface system (3.22) with the coefficient matrix

$$\mathscr{A} = \left(S_M(\frac{1}{2}A_x + \frac{1}{2}D_0 + \frac{1}{h_y}G)S_M - \frac{1}{h_y^2}(I_M + D_\alpha^{-1}D_\beta) \right).$$

In order to solve the system (3.22), we use

$$P = -\frac{1}{h_y^2}(I_M + D_\alpha^{-1}D_\beta)$$

as a preconditioner. The preconditioned interface system is defined by

$$\mathscr{A}P^{-1}v = \hat{b} \quad \text{and} \quad P\bar{u}_{:,N+1} = v, \tag{3.34}$$

where

$$\hat{b} = \frac{1}{2}S_M f_{:,N+1} - \frac{1}{h_y}S_M g - \frac{1}{h_y^2}D_\alpha^{-1}\hat{f}_{:,N}.$$

We use the BiCG method to solve the linear system (3.34). As usual, the iteration stops when

$$\frac{\|\hat{b} - \mathscr{A}P^{-1}v^p\|_2}{\|\hat{b} - \mathscr{A}P^{-1}v^0\|_2} \le \delta,$$

where v^p is the numerical solution at the pth iteration and v^0 is an initial value.

4. Numerical experiments

In this section, two examples of the cavity model are reported to test our algorithm. Numerical experiments are done only for the TM case. Our focus is on the accuracy and efficiency of the fast algorithm for solving the discrete linear systems. Throughout, the computation is performed on a Blade 1000 Sun-workstation in complex double precision. The BiCG method given in [6] is applied to solve the system (3.22). We always choose $\delta = h_x^2/5$.

The physical parameter of interest is the RCS, which is defined by

$$\sigma = \frac{4}{k_0}|P(\phi)|^2,$$

where ϕ is the observation angle and P is the far-field coefficient given by

$$P(\phi) = \frac{k_0}{2}\sin\phi \int_\Gamma u(x,0)e^{ik_0 x\cos\phi}\,dx\,.$$

Table 2: Errors for the fast algorithm (Example 4.1).

k_0	Error	Mesh			error order
		256×256	512×512	1024×1024	
4π	$e_M(\Gamma)$	5.742D-05	1.415D-05	3.367D-06	$h^{2.046}$
	$e_2(\Gamma)$	4.123D-05	1.015D-05	2.415D-06	$h^{2.047}$
	$e_M(\Omega)$	1.035D-04	2.569D-05	6.262D-06	$h^{2.023}$
	$e_2(\Omega)$	4.311D-05	1.067D-05	2.587D-06	$h^{2.029}$
8π	$e_M(\Gamma)$	1.344D-04	3.372D-05	8.452D-06	$h^{1.996}$
	$e_2(\Gamma)$	9.126D-05	2.284D-05	5.716D-06	$h^{1.999}$
	$e_M(\Omega)$	4.414D-04	1.092D-04	2.653D-05	$h^{2.028}$
	$e_2(\Omega)$	1.927D-04	4.767D-05	1.159D-05	$h^{2.028}$
16π	$e_M(\Gamma)$	6.466D-04	1.476D-04	3.687D-05	$h^{2.066}$
	$e_2(\Gamma)$	3.866D-04	9.542D-05	2.387D-05	$h^{2.009}$
	$e_M(\Omega)$	2.218D-03	5.177D-04	1.262D-04	$h^{2.068}$
	$e_2(\Omega)$	8.950D-04	2.086D-04	5.071D-05	$h^{2.071}$
32π	$e_M(\Gamma)$	2.340D-03	6.384D-04	1.594D-04	$h^{2.002}$
	$e_2(\Gamma)$	1.513D-03	4.118D-04	1.047D-04	$h^{1.976}$
	$e_M(\Omega)$	8.927D-03	2.315D-03	5.715D-04	$h^{2.018}$
	$e_2(\Omega)$	3.601D-03	8.862D-04	2.166D-04	$h^{2.032}$
4π	$e_M(\Gamma)$	2.153D-05	5.135D-06	1.191D-06	$h^{2.088}$
$\epsilon_r = 4+\mathrm{i}$	$e_2(\Gamma)$	1.546D-05	3.695D-06	8.583D-07	$h^{2.086}$
	$e_M(\Omega)$	2.185D-05	5.339D-06	1.280D-06	$h^{2.047}$
	$e_2(\Omega)$	8.104D-06	1.967D-06	4.682D-07	$h^{2.057}$
8π	$e_M(\Gamma)$	4.224D-04	1.036D-04	2.511D-05	$h^{2.036}$
Layered	$e_2(\Gamma)$	2.920D-04	7.165D-05	1.731D-05	$h^{2.038}$
Media	$e_M(\Omega)$	7.110D-04	1.765D-04	4.322D-05	$h^{2.020}$
(4.2)	$e_2(\Omega)$	2.479D-04	6.115D-05	1.487D-05	$h^{2.030}$
8π	$e_M(\Gamma)$	2.676D-04	6.566D-05	1.572D-05	$h^{2.044}$
Layered	$e_2(\Gamma)$	1.851D-04	4.534D-05	1.084D-05	$h^{2.046}$
Media	$e_M(\Omega)$	6.041D-04	1.499D-04	3.677D-05	$h^{2.019}$
(4.3)	$e_2(\Omega)$	1.800D-04	4.454D-05	1.088D-05	$h^{2.024}$

Example 4.1. We consider an artificial example defined by Eqs. (2.9)-(2.11) with a cavity $a = b = 1$ to verify the accuracy of approximations. The $f(x,y)$ and $g(x)$ are chosen such that the exact solution is

$$u(x,y) = (1+\mathrm{i})\sin\left(\frac{k_0 x}{2}\right)\sin\left(\frac{(k_0-\pi)(y+1)}{2}\right). \tag{4.1}$$

Since

$$g(x) = \frac{\partial u}{\partial n} - I(u)$$

cannot be given analytically, we evaluate $g(x)$ numerically. Four different cases to be tested are an empty cavity with $\epsilon_r(x,y) = 1.0$, and cavities filled with a complex homogeneous medium $\epsilon_r(x,y) = 4+\mathrm{i}$ and with two layered media defined by

$$\epsilon_{r_1}(x,y) = \begin{cases} 1.0, & -b/2 \le y < 0, \\ 4.0, & -b \le y < -b/2, \end{cases} \tag{4.2}$$

and

$$\epsilon_{r_2}(x,y) = \begin{cases} 1.0, & -b/2 \le y < 0, \\ 4+\mathrm{i}, & -b \le y < -b/2, \end{cases} \tag{4.3}$$

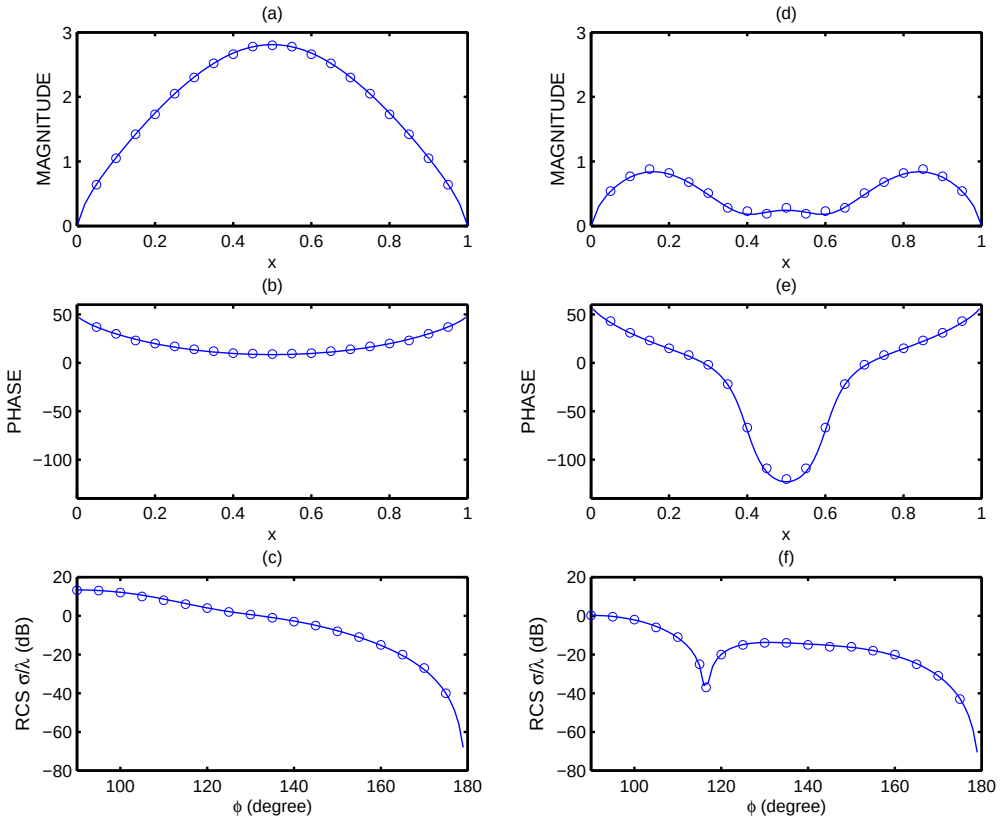

Figure 2: The magnitude and the phase of the aperture electric field at the normal incidence and the backscatter RCS for the rectangular cavity ($a = 1$m, $b = 0.25$m) for the TM case ($k_0 = 2\pi$). (a)-(c) for $\epsilon_r = 1.0$. (d)-(f) for $\epsilon_r = 4 + \mathrm{i}$ (Example 4.2).

respectively.

Error measures in L_2 norm and L_∞ norm in the domain Ω are defined by

$$e_2(\Omega) = \left(\frac{ab}{M(N+1)} \sum_{i,j=1}^{M,N+1} |u_{ij}^h - u(x_i, y_j)|^2 \right)^{1/2},$$

and

$$e_M(\Omega) = \max_{i,j} |u_{ij}^h - u(x_i, y_j)|,$$

respectively, where u_{ij}^h denotes the numerical solution at the point (x_i, y_j). Since the solution at the aperture of cavity (interface) is more important, we also define the following error measures on Γ,

$$e_2(\Gamma) = \left(\frac{a}{M} \sum_{i=1}^{M} |u_{i,N+1}^h - u(x_i, 0)|^2 \right)^{1/2},$$
$$e_M(\Gamma) = \max_i |u_{i,N+1}^h - u(x_i, 0)|.$$

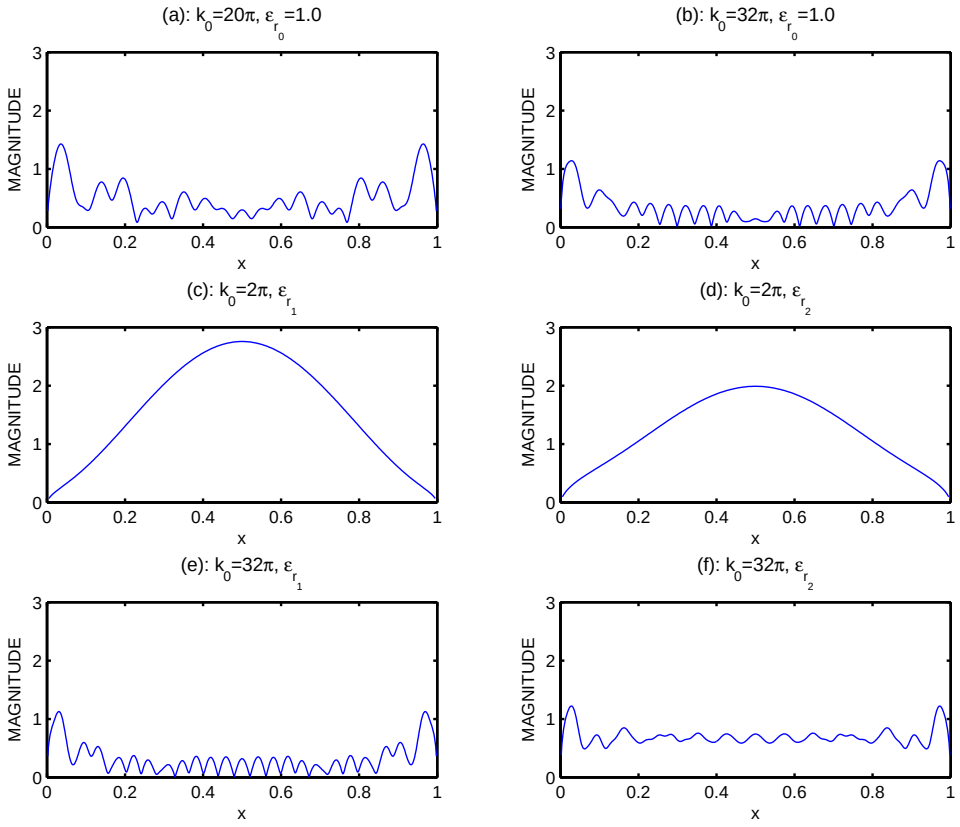

Figure 3: The magnitude of the aperture electric field for the cavity model with different k_0 and ϵ_r (Example 4.2).

We present numerical errors in Table 2 with different wavenumbers and different numbers of mesh points. Error orders are calculated by a least squares fit. Numerical results show that the numerical approximation has the second-order accuracy. Compared with the first-order algorithm proposed in [5], the present algorithm is more attractive, particularly for the cavity models with large wavenumbers.

Example 4.2. Consider a time-harmonic plane wave scattering from a rectangular cavity with 1 meter wide and 0.25 meter deep ($a = 1.0$ and $b = 0.25$) at normal incidence($\theta = 0$).

Above all, two different cases to be considered are an empty cavity with $\epsilon_r(x, y) = 1.0$, and a cavity filled with a homogeneous medium $\epsilon_r(x, y) = 4 + \mathrm{i}$. These two cases have been standard test problems in [8]. The case I was also tested in [5]. Here, we apply our fast algorithm to both the case I and the case II. In Fig. 2, we present the magnitude and the phase of the field, and the backscatter RCS for $k_0 = 2\pi$. These results are compared with numerical results (denoted by $'\mathrm{o}'$) presented in [8]. In addition, we solve the scattering problem from the empty cavities with large wavenumbers $k_0 = 20\pi$ and $k_0 = 32\pi$, respectively. We also solve the scattering problem from the cavities filled with the layered

Table 3: CPU time (sec.) and the number of iterations for the fast algorithm (Example 4.2).

k_0	No.of unknowns $(M \times N)$	CPU (Step (i))	CPU (Step (ii))	CPU (No. of Iteration) (Step (iv))	Total CPU
4π	256^2	1.0376E-03	3.3843E-02	3.0492E-02 (5)	6.6765E-02
	512^2	2.1526E-03	0.1354	7.888E-02 (6)	0.2197
	1024^2	4.1726E-03	0.56632	0.1685 (6)	0.7458
	2048^2	8.2473E-03	2.3778	0.4209 (7)	2.82245
8π	256^2	1.1394E-03	3.3867E-02	4.2774E-02 (7)	7.9159E-02
	512^2	2.3508E-03	0.1354	1.0489E-01 (8)	0.2458
	1024^2	4.5786E-03	0.5663	0.2247 (8)	0.8024
	2048^2	9.1090E-03	2.4058	0.5414 (9)	2.97206
16π	256^2	1.2050E-03	3.3870E-02	6.7223E-02 (11)	1.0368E-01
	512^2	2.4810E-03	0.1355	0.1575 (12)	0.2986
	1024^2	4.7207E-03	0.5663	0.3657 (13)	0.9436
	2048^2	9.5825E-03	2.3989	0.8445 (14)	3.26893
32π	256^2	1.2286E-03	3.3842E-02	0.1161 (19)	0.1526
	512^2	2.5502E-03	0.1355	0.2495 (19)	0.3907
	1024^2	4.9441E-03	0.5621	0.6748 (24)	1.2488
	2048^2	9.8800E-03	2.3511	1.3841 (23)	3.76070
4π	256^2	1.2100E-03	6.2091E-02	5.6450E-02 (9)	0.1225
$\epsilon_r = 4 + \mathrm{i}$	512^2	2.3478E-03	0.2480	0.1193 (9)	0.3761
	1024^2	4.2568E-03	0.9922	0.2819 (10)	1.2908
	2048^2	8.4978E-03	4.1814	0.6101 (10)	4.8267
8π	256^2	1.2596E-03	3.6616E-02	5.0036E-02 (8)	9.0710E-02
Layered	512^2	2.4076E-03	0.1373	0.1055(8)	0.2513
Media	1024^2	4.8382E-03	0.5485	0.2291(8)	0.7949
(4.2)	2048^2	9.4144E-03	2.3939	0.5620(9)	2.9918
8π	256^2	1.2682E-03	6.0296E-02	4.3273E-02(7)	0.1077
Layered	512^2	2.4108E-03	0.2239	9.3627E-02(7)	0.3264
Media	1024^2	4.6856E-03	0.9182	0.2262(8)	1.1618
(4.3)	2048^2	9.5114E-03	6.6129	0.4948(8)	7.1438

media (4.2) and (4.3) for $k_0 = 2\pi$ and $k_0 = 32\pi$, respectively. The magnitude of the aperture electric fields are shown in Fig. 3. Here, we see that the solutions of the cavity model with large wavenumbers are very oscillatory.

Finally, we present in Table 3 the CPU time at each step, the total CPU time, and the number of iterations in Step (iv) by the BiCG method until $N = M = 2048$. As shown in the table, the CPU time in Step (i) is proportional to M, which is the number of mesh points in the x-direction. The CPU time in Step (ii) is proportional to MN. It is obvious that the number of iterations in Step (iv) by the BiCG method is almost independent of the number of mesh points, and increases as the wavenumber remarkably. Numerical results consist with our analysis in Table 1, and illustrate that the computational complexity for the solution on the aperture is $\mathcal{O}(MN + 12pM\log M)$ for an $M \times N$ mesh.

5. Concluding remarks

We have presented a second-order method for the electromagnetic scattering from a rectangular open (layered) cavity in both TM and TE cases. In this method, a classical central finite difference is used for the discretization of Helmholtz equation and a second-order collocation type approximation is used for the hypersingular integral equation on

the aperture. The fast algorithm proposed in [5] is extended to solving the large finite difference system. The existence and uniqueness of numerical solutions are analyzed. The truncation error of the method is in the second order only when the solution is smooth. For many practical cases, the solution may have certain type singularities around corners and/or from the interface of two media. For the TE case, if $\epsilon_r(x, y)$ is discontinuous, some special technique developed for interface problems, such as IIM method [11], can be used to achieve the accuracy of the method. More importance is that a high-order approximation often provides a better resolution than a low-order approximation, particularly for those large cavity problems. In addition, we have also made some numerical simulations for the TE case, although only numerical results for the TM case have been presented here. Our numerical results for the TE case show many similar features. The number of iterations for the preconditioning algorithm is almost independent of the number of mesh points, while it depends upon the wavenumber k. Numerical simulations for more complicated media can be found in [18].

Acknowledgments The authors would like to thank the referees for their valuable suggestions. The work was supported in part by a grant from the Research Grants Council of the Hong Kong Special Administrative Region, China (Project No. CityU 102204).

References

[1] H. Ammari, G. Bao and A.W. Wood, *Analysis of the electromagnetic scattering from a cavity*, Japan J. Indust. Appl. Math., 19(2002), pp. 301–310.

[2] H.T. Anastassiu, *A review of electromagnetic scattering snalysis for inlets, cavities, and open ducts*, IEEE Antennas Propag. Mag., 45(2003), pp. 27–40.

[3] A.K. Aziz, R.B. Kellogg and A.B. Stephen, *A two point boundary value problem with a rapidly oscillating solution*, Numer. Math., 53(1988), pp.107–121.

[4] I. Babuska and S.A. Sauter, *Is the pollution effect of the FEM avoidable for the Helmholtz equation considering high wave number?*, SIAM J. Numer. Anal., 34(1997), pp. 2392–2423.

[5] G. Bao and W. Sun, *A fast algorithm for the electromagnetic scattering from a large cavity*, SIAM J. Sci. Comput., 27(2005), pp. 553–574.

[6] R.H. Chan and M.K. Ng, *Conjugate gradient methods for Toeplitz systems*, SIAM Rev., 38(1996), pp. 427–482.

[7] S.C. Hawkins, K. Chen and P.J. Harris, *On the influence of the wavenumber on compression in a wavelet boundary element method for the Helmholtz equation*, Int J. Numerical Analysis & Modeling, 4(2007), pp.48-62.

[8] J.M. Jin, *The Finite Element Method in Electromagnetics*, second ed., John Wiley & Sons, New York, 2002.

[9] X.Q. Jin, *Developments and Applications of Block Toeplitz Iterative Solvers*, Science Press & Kluwer Academic Publishers, Beijing/New York, 2002.

[10] R. Lee and T.T. Chia, *Analysis of electromagnetic scattering from a cavity with a complex termination by means of a hybrid ray-FDTD method*, IEEE Trans. Antennas Propag., 41(1993), pp. 1560–1569.

[11] R.J. LeVeque and Z. Li, *The immersed interface method for elliptic equations with discontinuous coefficients and singular sources*, SIAM J. Numer. Anal., 31(1994), pp. 1019–1044.

[12] J. Liu and J.M. Jin, *A highly effective preconditioner for sovling the finite element-boundary integral matrix equation of 3-D scattering*, IEEE Trans. Antennas Propag., 50(2002), pp. 1212–1221.
[13] P.R. Rousseau and R.J. Burkholder, *A hybrid approach for calculating the scattering from obstacles within large, open cavities*, IEEE Trans. Antennas Propag., 43(1995), pp. 1068–1075.
[14] W. Sun and J.M. Wu, *Newton-Cotes formulas for numerical evaluation of certain hypersingular integrals*, Computing, 75(2005), pp. 297–309.
[15] J.W. Thomas, *Numerical Partial Differential Equations: Conservation Laws and Elliptic Equations*, Springer, New York, 1999.
[16] T. Van and A.W. Wood, *A time-domain finite element method for Helmholtz equations*, J. Comput. Phys., 183(2002), pp. 486–507.
[17] C.F. Wang and Y.B. Gan, *2D cavity modeling using method of moments and iterative solvers*, Progress In Electromagnetics Research, PIER, 43(2003), pp. 123–142.
[18] Y. Wang, *Preconditioning Iterative Algorithms for Electromagnetic Scattering from Large Cavities*, PhD thesis, City University of Hong Kong, 2007.
[19] Y. Wang, K. Du and W. Sun, *Preconditioning Iterative algorithms for solving electromagnetic scattering from a large cavity*, Numerical Linear Algebra & Applications (to appear).
[20] W.D. Wood and A.W. Wood, *Development and numerical solution of integral equations for electromagnetic scattering from a trough in a ground plane*, IEEE Trans. Antennas Propag., 47(1999), pp. 1318–1322.
[21] J.M. Wu and W. Sun, *The superconvergence of trapezoidal rule for Hadamard finite part integrals*, Numer. Math., 102(2005), pp. 343–363.
[22] J.M. Wu and W. Sun, *The superconvergence of Newton-Cotes quadrature for Hadamard finite-part integrals on interval*, Numer Math, 109(2008), pp. 143-165.
[23] J.M. Wu, Y. Wang, W. Li and W. Sun, *Toeplitz-type approximations to the Hadamard integral operators and their applications in electromagnetic cavity problems*, Appl. Numer. Math., 58(2008), pp. 101–121.
[24] Z. Xiang and T.T. Chia, *A hybrid BEM/WTM approach for analysis of the EM scattering from large open-ended cavities*, IEEE Trans. Antennas Propag., 49(2001), pp. 165–173.